Adaptive Control Of A Single-Link Flexible Manipulator In The Presence Of Joint Friction And Load Changes

Vincente Feliu[1]
Robotics Institute
Carnegie Mellon University
Pittsburgh, Pennsylvania 15213

Kuldip S. Rattan
Department of Electrical Engineering
Wright State University
Dayton, OH. 45435

H. Benjamin Brown, Jr.
Robotics Institute
Carnegie Mellon University
Pittsburgh, Pennsylvania 15213

Abstract

A new method to control single-link lightweight flexible manipulators is proposed in this paper. The objective of this method is to control the tip position of the flexible manipulator in the presence of joint friction and changes in the payload. Both linear and nonlinear frictions are overcome using a very robust control scheme for flexible manipulators. The control scheme is based on two nested feedback loops: an inner loop to control the position of the motor and an outer loop to control the tip position. The compensation for changes in the load is achieved by decoupling the dynamics of the system and then applying a very simple adaptive control for the tip position. This results in a quite simple control law that needs minimal computing effort and thus can be used for real-time control of flexible arms.

1 Introduction

A major research effort has been made in the last five years to control flexible structures and, in particular, flexible arms. Several papers have appeared on the control of single-link flexible arms with a fixed payload at the tip [1-6]. Some adaptive control schemes have also been proposed to handle the problem of a changing payload [7-10]. However, very little effort has been devoted to the control of flexible arms when either Coulomb or dynamic friction is present in the joints, in spite of this case being very common in practice.

This paper presents a new control scheme that compensates for frictional effects and for undesired changes in the dynamics of the system caused by changes in the payload. This control method has been designed for the special case of lightweight (compared with the load that they handle) flexible arms. In this case the mechanical structure exhibits a dominant low frequency vibrational mode and negligible higher frequency modes.

Problems caused by Coulomb friction (which is a nonlinear component of the friction) as well as by the changes in the dynamic friction coefficient are overcome by using a general robust control scheme developed in [11]. This is composed of two nested loops: an inner loop that controls the position of motor and an outer loop that controls the tip position (See Fig. 1). In this figure $\theta_m(t)$ is the motor angle, $\theta(t)$ the tip position angle, and i the motor current.

A new scheme to adapt the control law to changes in the load is proposed. Adaptive controls referenced above are based on the Model Reference Adaptive Control (MRAC) [7,8] or on a two-stage process, a system identification stage followed by the adaptation of the controller as a function of the identified system parameters [9,10]. Both methods require a large amount of calculations to be performed in real-time and hence require relatively powerful computers. This restricts their use in controlling multi-link flexible arms. The adaptive control scheme proposed here is of the latter kind. It uses a decoupling scheme, developed in [12], that transforms the dynamic equations of the flexible arm into a simple double integrator system with only one parameter to estimate: the gain. This makes the identification stage very fast and the adaptation law very simple.

The control loop for the motor position is briefly described in Section 2. Section 3 describes the adaptive scheme for the tip position loop. Experimental results are shown in Section 4, and conclusions are drawn in Section 5.

2 Motor Position Control Loop

This control loop corresponds to the inner loop of Figure 1. We want to achieve two objectives when designing a controller for this loop:

1. to remove the modelling error and the nonlinearities introduced by Coulomb friction and changes in the coefficient of the dynamic friction,
2. to make the response of the motor position much faster than the response of the tip position control loop (outer loop in Figure 1).

[1] Visiting Prof., Dpto Ingenieria Electrica, Electronica y Control, UNED, Ciudad Universitaria, Madrid-28040, Spain.

The fulfillment of the second objective allows us to substitute the inner loop by an equivalent block whose transfer function is approximately equal to one, i.e., the error in motor position is small and is quickly removed. This simplifies the design of the outer loop as will be seen in the next section. The differential equation relating the angle of the motor to the applied current can be written as

$$Ki = J\frac{d^2\theta_m(t)}{dt^2} + V\frac{d\theta_m(t)}{dt} + Ct(t) + Cf(t) \qquad (1)$$

where K is the electromechanical constant of the motor, i is the current of the motor, $\theta_m(t)$ is the angle of the motor, J is the polar moment of inertia of the motor and hub, V is the dynamic friction coefficient, Ct(t) is the coupling torque between the motor and the link (the bending moment at the base of the link), Cf(t) is the Coulomb friction and t is time.

To simplify the design of the inner loop, the system described in equation (1) can be linearized by compensating for the Coulomb friction and can be decoupled from the dynamics of the beam by compensating for the coupling torque. This is done by adding, to the control current, the current equivalent to these torques and is given by

$$i_c(t) = (Ct(t) + Cf(sign\ of\ motor\ velocity))/K \qquad (2)$$

The coupling torque Ct(t) can be calculated either from strain gauge measurements at the base of the link, or by the difference of the measurements of the angles of motor and tip. The second approach is used here. Because the beam is nearly massless, we can assume that $Ct(t) = C(\theta_m(t) - \theta_t(t))$, where C is the stiffness of the arm. After compensating for the friction and coupling torque, the transfer function between the angle of the motor and the current is given by

$$\frac{\theta_m(s)}{i(s)} = G_m(s) = \frac{K/J}{s(s + V/J)} \qquad (3)$$

The block diagram of the inner loop control system is shown in Figure 2 (discrete control version). The feedforward and feedback controllers (G_{c1} and G_{c2} respectively) are designed so that the response of the inner loop (position control of the motor) is significantly faster than the response of the outer loop (position control of the tip) and without any overshoot. This is done by making the gain of the feedforward controller large and is limited only by the saturation current of the servo amplifier. It was shown in [11] that, in theory, this gain could be made arbitrarily large even in the case of the arm being a nonminimum phase system. It was also shown also that large gains in this loop reduce the effects of nonlinearities caused by friction.

When the closed-loop gain of the inner loop is sufficiently high, the motor position will track the reference position with small error. The dynamics of the inner loop may then be approximated by '1' when designing the outer loop controller.

3 Tip Position Adaptive Controller

Provided that the inner loop has been satisfactorily closed, the dynamics of the arm ($G_b(s)$ in Figure 1) are reduced to

$$G_b(s) = \frac{\omega_n^2}{s^2 + \omega_n^2} \qquad (4)$$

for the case of lightweight flexible arms. The natural resonant frequency of the beam with the motor fixed is ω_n rad/sec., and is related to the stiffness of the beam (C) and the load at the tip (m) by the expression

$$\omega_n^2 = \frac{C}{mL^2} \qquad (5)$$

where L is the length of the arm.

The proposed control scheme for the tip position is composed of three loops: a decoupling loop, a classical P.D. controller with a feedforward term (see Fig. 3), and an adaptation loop (shown in Fig. 4).

3.1 Decoupling loop

The purpose of this loop is to simplify the dynamics of the arm. For the case of a beam with only one vibrational mode, a very simple decoupling loop can be implemented that reduces the dynamics of the system to a double integrator. This is done by simply closing a positive feedback unity gain loop around the tip position. Thus, expression (4) is transformed into

$$G'(s) = \frac{\omega_n^2}{s^2} \qquad (6)$$

3.2 P.D. Controller

It is well known that the poles of a plant of the form (6) can be perfectly placed by using a simple P.D. controller [13]. Let us express this controller as

$$G_{c3}(s) = \frac{1}{\omega_n^2}(c_0 + c_1 s) \qquad (7)$$

A feedforward acceleration term may be added in order to make the tip follow the reference without any delay and is given by

$$Feedforward(s) = \frac{1}{\omega_n^2}s^2\theta_{tr}(s) \qquad (8)$$

where $\theta_{tr}(s)$ is the Laplace transform of the commanded trajectory profile for the tip. Notice that (8) uses the second derivative of the reference. It means that parabolic profiles of at least order two must be used as reference signals in this scheme.

The resulting control scheme after closing loops described in sections 3.1. and 3.2. is shown in Figure 3. If the load

at the tip were constant, this scheme would provide a nearly perfect trajectory tracking and error compensation for the tip position.

3.3 Adaptive control

Changes in the carried load produce changes in ω_n, deteriorating the dynamic performance. An adaptive controller is proposed here to overcome this. It consists of two parts: the first that identifies the gain of the system ω_n^2, and the second that changes the scaling block ,$1/\omega_n^2$, of the controller (see Fig. 3) to the new estimated value. Estimation of the parameter ω_n^2 is easily done by integrating the input, $x(t)$, twice, and then dividing the actual tip position by this value. Notice that

$$\frac{\theta_t(s)}{x(s)} = \omega_n^2/s^2 \rightarrow \hat{\omega_n^2} = \frac{\theta_t(s)}{(x(s)/s^2)} \tag{9}$$

where $\hat{\omega_n^2}$ refers to the estimate. A scheme of the tip controller which includes the adaptive law (3rd tip position loop) is shown in Figure 4. Notice that the gain of the plant can be estimated easily due to having previously decoupled the system (in Subsection 3.1). The tuning law for the controller (which consists of the scaling block of Figure 4) is also very simple because of this reason.

4 Experimental Results

In this section, we first describe the experimental setup of a one-link lightweight flexible manipulator built in our laboratory. Next, the experimental results obtained from our control scheme are presented.

4.1 Experimental Setup

The mechanical system consists of a dc motor, a slender link attached to the motor hub, and a mass at the end of the link floating on an air table. Figure 5 shows the major parts of the system. The link is a piece of music wire (7 inches long and 0.032 inch in diameter) clamped in the motor hub. The tip mass is a 1/16 inch thick, 5 $\frac{3}{4}$ inch diameter fiberglass disk attached at its center to the end of the link with a freely pivoted pin joint. The disk has a mass of 54 gms and floats on the horizontal air table with minimal friction. Since the mass of the link is small compared to that of the disk, and because the pinned joint prevents generation of torque at the end of the link, the mechanical system behaves practically like an ideal, single degree-of-freedom, undamped spring-mass system.

A direct drive motor drives the link. The motor is powered by a 40V power supply through a DC servo amplifier. The amplifier current limit is set to 4.12 amps. , which corresponds to 9 lb. inch motor torque. Coulomb friction of the motor is about 0.288 lb. inch (corresponding to 0.132 amps) and has a significant effect on the control when the torque applied to the arm is low, as with our slender arm. The system was designed to give tip response much slower than the motor response. Mechanical stops limit the travel of the motor and the hub to about ± 27 degrees.

Two sensors are used for the control of the system. A 7/8 inch, 360 degree potentiometer provides the angle of the motor shaft. A Hamamatsu tracking camera (with an infrared filter) senses the X-Y position of an infrared LED mounted on the tip of the arm. The workspace of the arm is limited to about ± 3 inch (± 25 degrees) by the field of view of the camera.

The control algorithm is implemented on an MC68000-based computer with 512K bytes of dynamic RAM and a 10 MHZ clock. Analog interfacing is provided with 12 bit A/D and D/A boards. Switch signals for starting and stopping control routines, as well as other functions, are read through parallel I/O ports. As floating point operations are slow (approximately 0.5 msec. per multiplication), real-time computations are done in integer (approximately 0.08 msec. per multiplication) or short integer (0.02 msec.) arithmetic. A matrox graphics interface card permits the display of data on a 12 inch monitor.

Using an identification technique described in [14] we determine the parameters of the arm to be

J = 0.005529 lb.$in.sec^2$
V = 0.01216 lb.in./rad./sec.
K = 2.184 lb.in./amp.
Coulomb friction = 0.2883 lb.in (0.132 amp.)
Ct(t) = C($\theta_m(t) - \theta_t(t)$), C = 0.674 lb.in./rad..

and the transfer function of the beam is given by

$$G_b(s) = \frac{43.75}{s^2 + 43.75} \tag{10}$$

The estimated value of the Coulomb friction corresponds to an equivalent torque generated by a beam deflection of 25 degrees, so its effect is very noticeable.

4.2 Inner loop control design

The inner loop incorporates compensation terms for Coulomb friction and the coupling between the motor and the beam, according to (2). The scheme of Figure 2 is used for the inner loop. A delay term is included in the scheme in order to take into account the delay in the control signal because of the computations. A sampling period of 3 msec. is used for this inner loop.

An optimization program was developed to get the best controllers using the model obtained for the motor. The settling time (considering an error of less than 1%) of the response of the motor to step commands in the motor angle

reference input was minimized. The saturation limit of the current amplifier was also taken into account in this design. Step inputs were assumed as references for the inner loop because, in order to get a good control action, the command angle for the motor should experience very sharp changes. In fact, in our experiments, the motor angle varied much faster than the angle of the tip. The resulting controllers were

$$G_{c1}(z) = 17.442 - 2.442z^{-1}$$

$$G_{c2}(z) = 6.667 - 5.667z^{-1}$$

Figure 7 shows the response of the motor position to a step change in its reference keeping the tip of the arm fixed in the zero angle position. This means that, in the steady-state of this experiment, there is always a coupling torque Ct caused by the bending of 200 mrad existing between the angle of the motor and the angle of the tip. The zero steady-state error shown by the experimental data demonstrates the effectiveness of compensation achieved for the Coulomb friction and for the coupling of the motor with the beam. The settling time achieved for the motor is 33 msec. which is significantly faster than the dynamics of the beam. This allows us to assume that the equivalent transfer function of the inner loop is 1.

4.3 Outer loop control design

We first design the controller $G_{c3}(s)$ of Figures 3 and 4 for the case of the load being 54 gms.. Designing an analog P.D. controller and then discretizing it using the Tustin transform [15], we get the digital controller

$$G_{c3}(z) = 3281.25(\frac{1 - 0.987z{-}1}{1 - 0.74z^{-1}}) \qquad (11)$$

4.4 Adaptation

The adaptation scheme described in Subsection 3.3. is used. Experimental results are shown in Figures 8-11. Parabolic profiles of order 2 are given to the controller as references for the tip position. Comparisons between the responses of the arm when using the nominal controller (9) (block $1/\omega_n^2$ of Figure 4 is held constant at the value corresponding to a load of 54 gm.) and when using the adaptive controller (block $1/\omega_n^2$ is tuned) are presented. Figure 8 shows the response of the system with the nominal payload of 54 gm. and the nominal controller (non-adaptive). Notice that the response is very good because G_{c3} was designed for these conditions. Figure 9 shows the adaptive response with the nominal payload. Figure 10 shows both adaptive and non-adaptive responses when payload is 142 gm., and Figure 11 when the payload is 15.73 gm. . Notice that the system without the adaptive controller becomes unstable in the last case.

5 CONCLUSIONS

A new method to control single-link lightweight flexible arms in the presence of joint friction and changes in the load has been presented. Effects of nonlinear friction are removed by closing a high gain loop around the motor position. This was developed in a previous paper [11] and includes compensating terms for the coupling torque and for Coulomb friction.

A new method to control the tip position of the arm when there are changes in the tip load is presented in this paper. The method first decouples the dynamics of the system by closing a unity positive feedback loop around the tip position, and then an adaptive controller is designed for the decoupled system. This decoupling presents the advantage of making the adaptive control very simple.

The general control scheme is shown to be simple and computationally efficient : the sampling period was 3 msec. in our experiments, which was the time needed by real-time control calculations. The controller is composed of three nested control loops plus an adaptation loop, but each one consists of very simple elements. In fact, our experiments show that using a computer of very modest capabilities, a controller that fulfills the desired specifications can be implemented. The experimental responses were shown to be good even in the case of extreme conditions, the Coulomb friction was very high and changes in the payload were about 3 times more and less than the nominal load of 54 gms..

Another advantage, from the design point of view, is that each loop is designed independently (starting from the inner loop) and their elements are calculated easily and according to simple specifications. The inner loop is designed to compensate for friction and make the motor response fast. Both goals are achieved with the same high gain P.D. controller. The middle loop decouples the dynamics of the system (reduces its transfer function to a double integrator). The outer loop gives a fast and accurate response of the tip position (a simple P.D. with a feedforward term). The adaptive controller takes care of changes in the load by estimating only one parameter of the system.

Finally, this control approach is different from others in that the existing methods to control flexible arms are based on explicit control of the tip position, where the controller generates the current for the D.C. motor of the joint as a control signal. The proposed method is based on the simultaneous explicit control of the joint motor position and tip position. The controller for the motor position generates a control signal that is a current for the D.C. motor, like in the other existing methods, while the tip position controller generates a control signal which is a motor position reference for the inner loop.

REFERENCES

1. Robert H. Cannon and E. Schmitz, "Precise Control of Flexible Manipulators", Robotics Research, 1985.

2. Maria De and B. Siciliano "A Multilayer Approach to Control of a Flexible Arm", Proceedings 0f 1987 IEEE International Conference on Robotics and Automation. Raleigh (USA), April 1987.

3. F. Matsuno, S. Fukushima and coworkers, "Feedback Control of a Flexible Manipulator with a Parallel Drive Mechanism", International Journal of Robotics Research, Vol. 6, No. 4, Winter 1987.

4. J. C. Ower and Vegte J. Van de, "Classical Control Design for a Flexible Manipulator: Modeling and Control System Design", IEEE Journal of Robotics and Automation, Vol. RA-3, No. 5, October 1987.

5. F. Pfeiffer and B. Gebler, "A Multistage Approach to the Dynamics and Control of Elastic Robots", Proceedings 1988 IEEE International Conference on Robotics and Automation, Philadelphia (USA), April 1988.

6. T. Kotnick, S. Yurkovich and U. Ozguner, "Acceleration Feedback for Control of a Flexible Manipulator Arm", Journal of Robotic Systems, Vol. 5, no. 3, June 1988.

7. B. Siciliano, B. S. Yuan and W. J. Book, "Model Reference Adaptive Control of a One Link Flexible Arm", 25th IEEE Conference on Decision and Control, Athens, December 1986.

8. J. Yuh, "Application of Discrete-Time Model Reference Adaptive Control to a Flexible Single-Link Robot", Journal of Robotic Systems, Vol. 4, No. 5, 1987.

9. F. Harahima and T. Ueshiba, "Adaptive Control of Flexible Arm using the End-Point Position Sensing", Proceedings Japan-USA Symposium of Flexible Automation, Osaka (Japan), July 1986.

10. D. M. Rovner and R. H. Cannon, "Experiments Towards on-line Identification and Control of a Very Flexible One-Link Manipulator", International Journal of Robotics Research, Vol. 6, No. 4, Winter 1987.

11. Kuldip S. Rattan, V. Feliu and H. B. Brown, "A Robust Control Scheme for a Single-Link Flexible Manipulator with Friction in the Joints", Proceedings 2nd Annual USAF/NASA Workshop on Automation and Robotics, Dayton (USA), June 1988.

12. Kuldip S. Rattan, V. Feliu and H. B. Brown, "Experiments to Control Single-Link Lightweight Flexible Manipulators with One Vibrational Mode", Proceedings ISA International Conference on Robotics and Expert Systems, Houston (USA), October 1988.

13. B. C. Kuo, "Automatic Control Systems", Prentice-Hall, 1982.

14. V. Feliu, K. S. Rattan and H. B. Brown, "Model Identification of a Single-Link Flexible Manipulator in the Presence of Friction", Proceedings of 19th ISA Annual Modelling and Simulation Conference, Pittsburgh, May 1988.

15. H. F. VanLandingham, "Introduction to Digital Control Systems". MacMillan Publishing Company. 1985.

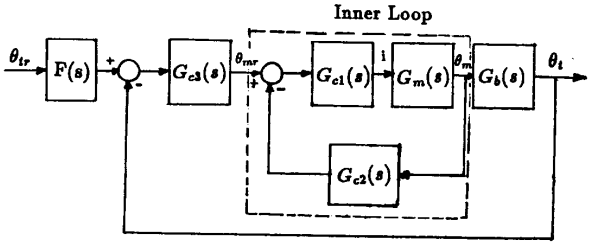

Figure 1. General Robust Control Scheme for Flexible Manipulators.

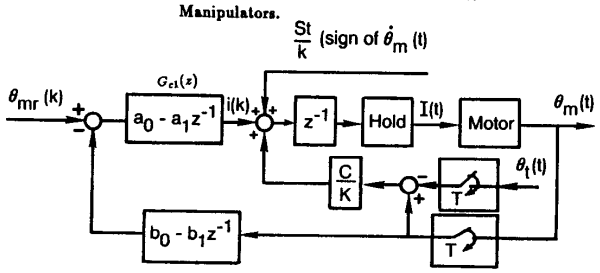

Figure 2. Inner Loop Control System.

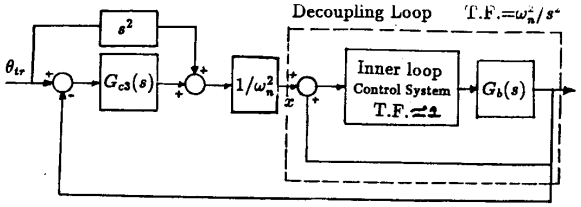

Figure 3. Tip Position Control Loop.

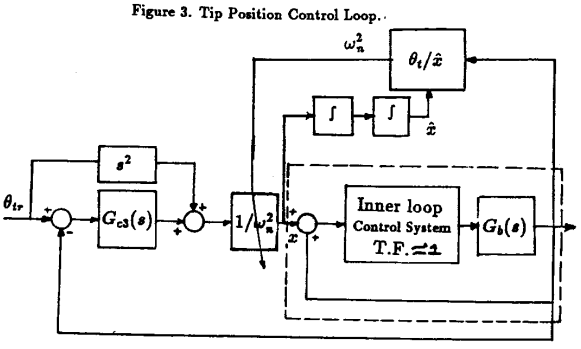

Figure 4. Adaptive Tip Position Control Loop.

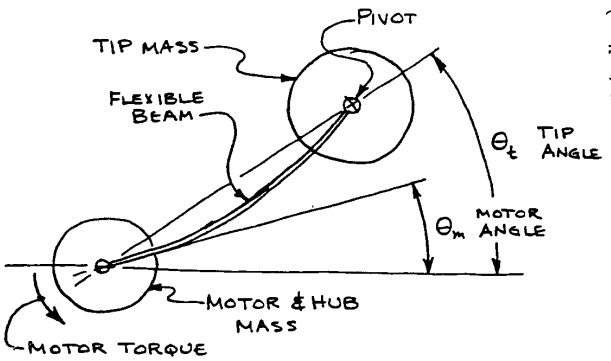

Figure 5. Experimental Setup.

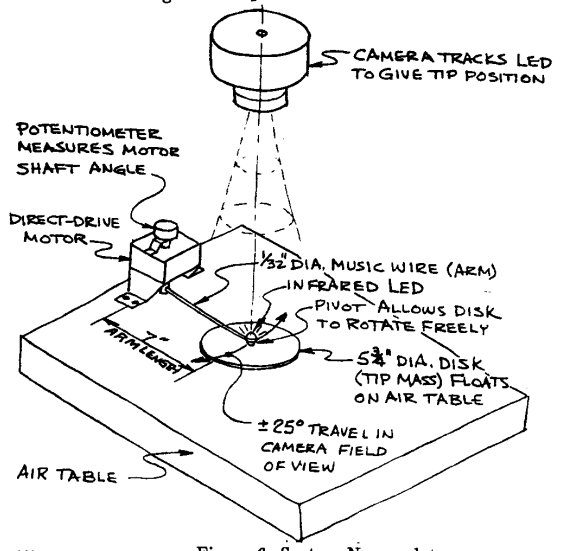

Figure 6. System Nomenclature

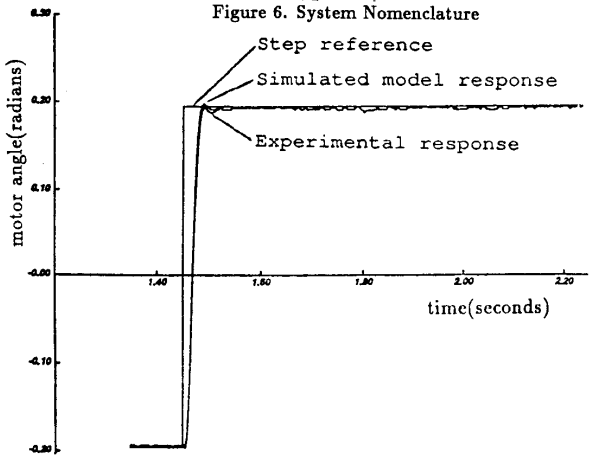

Figure 7. Experimental Response of the Inner Loop to a Step Input Command.

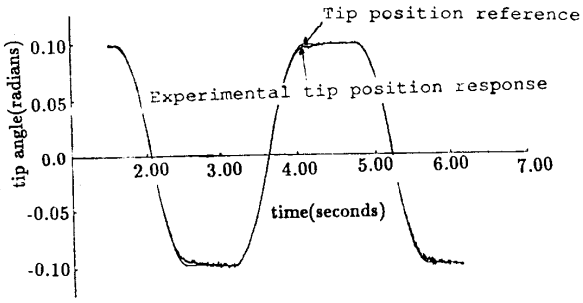

Figure 8. Tip Position Response with the Nominal Controller and a Payload of 54 gm.

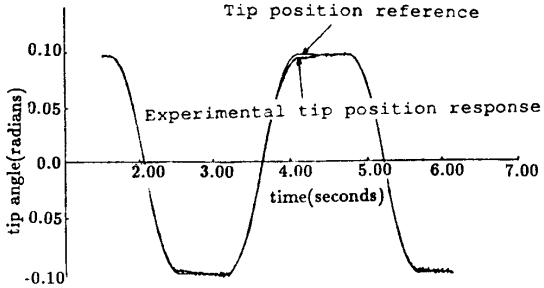

Figure 9. Tip Position Response with the Adaptive Controller and a Payload of 54 gm.

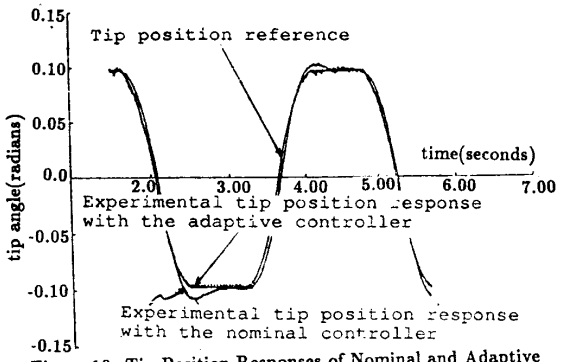

Figure 10. Tip Position Responses of Nominal and Adaptive Controllers (Payload of 142 gm).

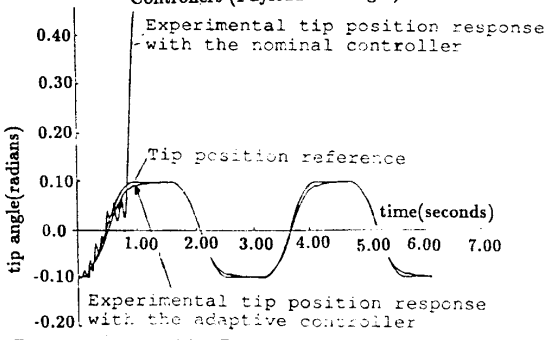

Figure 11. Top Position Responses of Nominal and Adaptive Controllers (Payload of 15.73 gm).